Two Dynamic Regimes of Finite Amplitude Charney and Green Waves*

BIN WANG

Geophysical Fluid Dynamics Program, Princeton University, Princeton, NJ 08542

ALBERT BARCILON

Meteorology Department and Geophysical Fluid Dynamics Institute, Florida State University, Tallahassee, FL 32306

(Manuscript received 20 May 1985, in final form 3 February 1986)

ABSTRACT

The weakly nonlinear evolutions of the Green and Charney waves are compared for two regimes: (1) when internal dissipation is the dominant dissipation; (2) when Ekman friction is the dominant dissipation.

When the Ekman dissipation is dominant, we obtain a large amplitude, equilibrated wave state which depends upon the initial conditions but not upon the magnitudes of the dissipation; the steady wave features a barotropic structure, and does not transport heat in the meridional direction. In sharp contrast, when internal dissipation is dominant, a small amplitude, equilibrated wave state is found, which is independent of the initial conditions but depends on the magnitude of the internal dissipation. The steady wave exhibits a westward phase tilt and transports heat poleward by an amount proportional to the internal dissipation.

The presence of a large planetary vorticity gradient stabilizes the finite amplitude evolution of the planetary waves and leads to a stable equilibrium planetary wave state.

1. Introduction

The different dynamic effects produced by thermal and mechanical dissipations in a linear analysis of an extended Charney model were found in a previous study (Wang, Barcilon, and Howard, 1985; henceforth denoted by WBH). It is of interest to further investigate the different roles they play in the finite amplitude evolutions of baroclinic waves.

The magnitudes of the Newtonian cooling and Ekman dissipation in quasi-geostrophic motion are proportional to the nondimensional numbers μ and δ, respectively, which are defined as

$$\mu = \frac{1}{f_0 R_0 \tau_*}, \tag{1.1}$$

$$\delta = S\frac{E^{1/2}}{R_0}, \tag{1.2}$$

where τ_* is the Newtonian cooling time, f_0 the Coriolis parameter, R_0, E, and S represent the Rossby number, Ekman number, and Burger number ($S = L_D^2/L^2$, where L_D and L are the radius of deformation and characteristic horizontal length scale, respectively). The weakly nonlinear analysis by Wang and Barcilon (1985, henceforth denoted by WB) considered the evolution of the most unstable Green mode in the presence of an $O(\Delta^{1/2})$ internal dissipation (mainly the Newtonian cooling) and an $O(\Delta)$ Ekman dissipation, where $\Delta \ll 1$ is a measure of the supercritical baroclinity. Physically, this regime implies that the Newtonian cooling time is of the same order of magnitude as the baroclinic development time scale, and the Ekman dissipation time scale is much longer than the baroclinic development time scale. Yet, as shown by (1.1) and (1.2), both the parameters μ and δ are dependent of the characteristic length scale, L, i.e., μ increases, while δ decreases with increasing L. If waves of scale shorter than planetary scale are considered, we expect that Ekman dissipation to be more important than the internal thermal damping. Therefore, we propose to reconsider the dynamics in the parameter region in which Ekman dissipation is dominant compared to the internal dissipation which in this paper will be due to Newtonian cooling, i.e., $\delta = O(\Delta^{1/2})$ and $\mu = O(\Delta)$; this study is an extension of Pedlosky (1979).

For ease of discussion we label the regime where internal dissipation is dominant, i.e., $\mu = O(\Delta^{1/2})$ and $\delta = O(\Delta)$, as Regime I, and label the regime where Ekman dissipation is dominant, i.e., $\delta = O(\Delta^{1/2})$ and $\mu = O(\Delta)$, as Regime II. As shown in section 4, we find rather different equilibrium wave states in these two regimes, one resembling a high index flow (Regime I), and the other resembling a low index flow (Regime II). In order to facilitate comparison with WB's results we develop the analysis in sections 2 and 3 for strongly unstable Green modes; however, the conclusion, summarized in section 4, regarding the different dynamic

* Contribution No. 230 of Geophysical Fluid Dynamics Institute, Florida State University, Tallahassee, Florida.

effects of the Newtonian cooling and Ekman dissipation are, in principle, equally applicable to the Charney mode.

Pedlosky (1979) found that, in the presence of an $O(\Delta^{1/2})$ Ekman dissipation and in the absence of Newtonian cooling, the Charney mode with wavelength of planetary scale exhibited a weak, frictionally induced, nonlinear instability. When a realistic planetary vorticity gradient is present, these planetary scale waves (wave two through four) fall in the unstable Green mode region. Section 5 compares the finite amplitude dynamics of the Charney mode with that of the Green mode for a fixed wavelength; the comparison will help understand the role of a realistic β-effect on the evolution of baroclinic waves.

2. Amplitude equations for the Green modes in regime II

The model used here is the same as the one used by WB, except that the minor horizontal diffusion of vorticity is ignored, and the internal dissipation coefficient $\mu = O(\Delta)$ is assumed to be much smaller than the Ekman dissipation coefficient $\delta = O(\Delta^{1/2})$, i.e., the Ekman spindown time is of the same order of magnitude as, while internal dissipation time is much longer than, the e-folding time of the baroclinic growth. The interested reader is referred to WB for the details of the model. After introducing a slow time scale $T = \Delta^{1/2}t$, the governing equation for strongly unstable *Green modes*, in the presence of Newtonian cooling, becomes

$$\left(\Delta^{1/2}\frac{\partial}{\partial T} + z\frac{\partial}{\partial x}\right)q + (4\tilde{K} - 2\tilde{K}\Delta)\frac{\partial\phi}{\partial x} + J(\phi, q) + \mu\left(\frac{\partial^2}{\partial z^2} - \frac{\partial}{\partial z}\right)\phi = 0, \quad (2.1)$$

where

$$q \equiv \left(\frac{\partial^2}{\partial z^2} - \frac{\partial}{\partial z} + S\nabla^2\right)\phi, \quad (2.1a)$$

is the perturbation potential vorticity, $K = (k^2 + l^2 + \frac{1}{4})^{1/2}$ is the modified total horizontal wavenumber, k and $l = (m + \frac{1}{2})\pi$, $m = 0, 1, 2, \cdots$, are nondimensional zonal and meridional wavenumbers, respectively. All the boundary conditions for ϕ remain identical to those used by WB.

The asymptotic solutions obtained by a singular perturbation technique can be summarized as follows. To $O(\epsilon^{3/2})$, the perturbation streamfunction is

$$\phi(x, y, z, T) = \epsilon^{1/2}e^{pz}\left[A(T)z(1 - \tilde{K}z) - \Delta^{1/2}\frac{i}{k}\frac{dA}{dT}(1 - 2\tilde{K}z)\right]\cos kx \cos ly + O(\epsilon^{3/2}), \quad (2.2)$$

where $\epsilon = O(\Delta)$ is an expansion parameter that measures the nonlinearity, and

$$p = \frac{1}{2} - \tilde{K} < 0 \quad (2.2a)$$

denotes the exponential decay rate of the wave amplitude with height. The zonal mean flow can be expressed as

$$\bar{u}(y, z, T) = z + \sum_{J=1}^{\infty}[B_J(T)e^{r_J z} + (|A(T)|^2 - |A(0)|^2)f_J(z)]\cos jy + O(\epsilon^{3/2}), \quad (2.3)$$

where $j = (J - \frac{1}{2})\pi$, $J = 1, 2, 3, \cdots$; $B_J(T)$ satisfies

$$\frac{dB_J}{dT} - \frac{j^2\delta}{\Delta^{1/2}r_J}B_J = (r_J - G_J)\frac{j^2\delta}{\Delta^{1/2}r_J^2}(|A(T)|^2 - |A(0)|^2), \quad (2.4)$$

$$B_J(0) = 0, \quad J = 1, 2, 3, \cdots.$$

In (2.3) and (2.4) $f_J(z)$, G_J, and r_J are defined by (A1), (A4a) and (A4b), respectively, in the Appendix; the evolution of the amplitude A is governed by

$$\frac{d^2A}{dT^2} + \tilde{\delta}\frac{dA}{dT} - \frac{k^2C_{0I}^2}{\Delta}\left(1 + i\frac{\mu SK^2}{z\Delta k\tilde{K}}\right)A + A[\chi(|A(T)|^2 - |A(0)|^2) + \sum_{J=1}^{\infty}\chi_J B_J] = 0, \quad (2.5)$$

where

$$\tilde{\delta} = \delta\frac{K^2}{\Delta^{1/2}(\tilde{K} - p)}, \quad (2.5a)$$

$$C_{0I} = \frac{\Delta^{1/2}}{[4\tilde{K}(\tilde{K} - p)]^{1/2}} \quad (2.5b)$$

is the imaginary part of the complex phase speed for inviscid Green modes, the quantities χ and χ_J that are involved in the wave–mean flow interaction term are respectively given by (A5) and (A6) in the Appendix.

There are two noticeable differences between the preceding amplitude equations, Regime II, and those for Regime I (WB). As a major damping factor, the $O(\Delta^{1/2})$ Ekman dissipation in Regime II exhibits its influence on the mean flow correction via the matching condition, so that the variation of the mean flow is governed by an infinite set of differential equations for each Fourier component, and the corresponding dynamic system can no longer be cast into a simple Lorenz set. Besides, an $O(\Delta)$ Ekman dissipation in Regime I does not affect the amplitude equation, yet an $O(\Delta)$ Newtonian cooling in Regime II does by appearing as an imaginary part of the coefficient of A [see (2.5)] in the wave amplitude equation, implying, as will be shown shortly, a weakly nonlinear destabilization.

To illustrate the time evolution and study some of the characteristics of these amplitude equations we performed numerical calculations, in which, (in 2.3), we truncated the infinite summations at $J = 10$; a Mersen scheme with adjustable time step was used to ensure

an accuracy of 10^{-5}. Repeated attempts to find (numerically) limit cycles and chaotic behaviors failed. Figure 1 shows a typical time evolution of the wave amplitude in the presence of $O(\Delta^{1/2})$ Ekman dissipation and $O(\Delta)$ internal dissipation. The wave grows, exhibiting a damped vacillation, then reaches an equilibrium state which describes a large amplitude, steady, propagating wave state that will be studied in greater details in the next two sections.

The vacillatory behavior occurring during the approach to steady wave states disappears if the dissipative time scale is shorter than the baroclinic development time scale. This is a common feature for both regimes. In Regime I, a rapid monotonic approach to the steady wave state would take place when the internal dissipation time scale is shorter than $\sqrt{3}/2$ times the e-folding time for baroclinic development (WB). In the Martian atmosphere, Newtonian cooling time is usually comparable to the baroclinic development time (Barnes, 1984), implying that after a relatively short period of development, baroclinic waves reach their steady states. This could be one of the relevant mechanisms responsible for the features of Martian circulation, where the weather variations, associated with travelling baroclinic waves, are much more regular in terms of the amplitude than those in the Earth's atmosphere (Leovy, 1979).

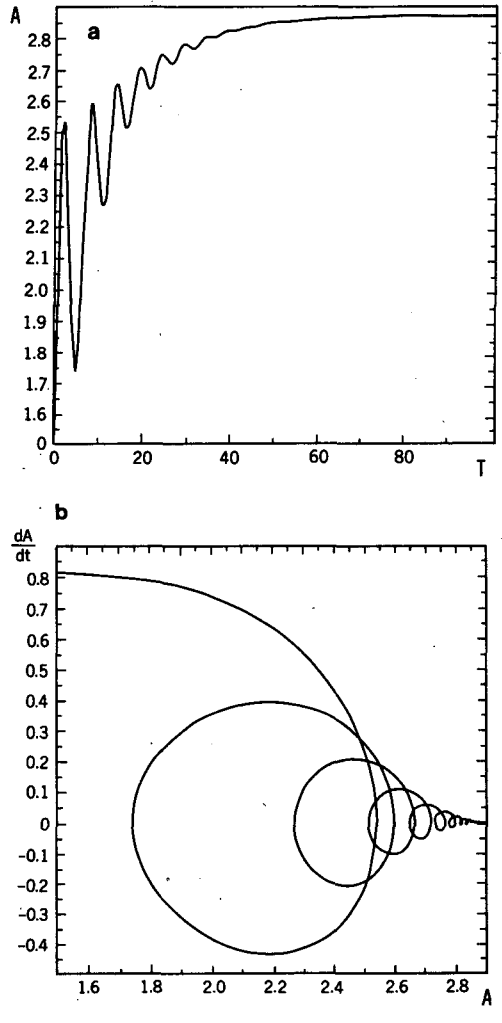

FIG. 1. (a) Time history of the wave amplitude in Regime II showing the approach to steady state with damped oscillation. The parameters used in calculation are: $k = 1.1$ (wave two), $l = \pi/2$, $\tilde{\delta} = 0.1$, $\Delta = 0.1$, $2\mu/\Delta = 0.03$. (b) The phase-plane orbit of the solution of (a).

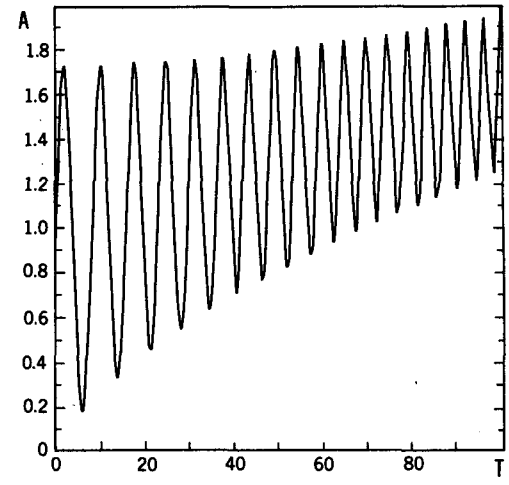

FIG. 2. The evolution of the amplitude $A(T)$ showing finite-amplitude instability induced by the small Newtonian cooling only. ($k = 1.1$, $l = \pi/2$, $\Delta = 0.1$, $2\mu/\Delta = 0.06$, $\delta = 0$).

If the Ekman dissipation is absent, and for $O(\Delta)$ internal dissipation Fig. 2 shows the evolution of the wave amplitude which displays finite-amplitude instability. WBH showed that in the immediate vicinity of the critical points $b = 4\tilde{K}$, the weak internal dissipation destabilizes the wave-free zonal flow in the linear dynamics. The behavior shown in Fig. 2 indicates that this destabilization survives in the nonlinear regime, and leads to catastrophy if we do not introduce Ekman dissipation or Newtonian cooling on a longer time scale.

3. Steady wave solutions and their stabilities

Equations (2.4) and (2.5) are suited for numerical integration. However, it is difficult to use (2.4) and (2.5) to examine the stability of the steady wave states analytically. We, therefore, make the transformation

$$\tilde{B}_J(T) = B_J(T) + (|A(T)|^2 - |A(0)|^2)(\mathcal{S}_0 - G_J) \quad (3.1)$$

then, the $O(\epsilon)$ mean flow correction becomes

$$\bar{u}_1(y, z, T) = \sum_{J=1}^{\infty} [\tilde{B}_J(T)e^{r_J z} + (|A(T)|^2 - |A(0)|^2)\tilde{f}_J(z)] \cos jy \quad (3.2)$$

where $\tilde{B}_J(T)$ satisfies

$$\frac{d\tilde{B}_J}{dT} - \frac{j^2\delta}{\Delta^{1/2}r_J}\tilde{B}_J = (\mathcal{S}_0 - G_J)\frac{d|A|^2}{dT}, \qquad (3.3)$$

and $\tilde{f}_J(z)$, G_J, and r_J are defined by (A2), (A4a), and (A4b), respectively. The corresponding wave amplitude equation (2.5) becomes

$$\frac{d^2A}{dT^2} + \tilde{\delta}\frac{dA}{dT} - \frac{k^2C_{0I}^2}{\Delta}\left(1 + i\frac{\mu SK^2}{2\Delta k\tilde{K}}\right)A + A[\tilde{\chi}(|A|^2 - |A(0)|^2) + \sum_{J=1}^{\infty}\chi_J\tilde{B}_J] = 0. \qquad (3.4)$$

where $\tilde{\chi}$, χ_J are given in the Appendix by (A7) and (A6).

The trivial steady solution $A = \tilde{B}_J = 0$ to (3.3) and (3.4) corresponds to the zonal baroclinic flow of the original basic state. Let $A', B'_J \sim e^{\Gamma T}$ be the small perturbations about that solution. The eigenvalues are given by

$$\Gamma_{1,2} = -\frac{\tilde{\delta}}{2} \pm \left[\frac{\tilde{\delta}^2}{4} + \frac{k^2C_{0I}^2}{\Delta}\left(1 + i\frac{\mu SK^2}{2\Delta k\tilde{K}}\right)\right]^{1/2},$$

$$\Gamma_k = \frac{(k - 5/2)^2\pi^2\delta}{r_{k-2}\Delta^{1/2}} < 0, \quad k = 3, 4, \cdots.$$

It can be shown that $\mathrm{Re}\Gamma_1 > 0$ implying that this equilibrium solution is always *unstable*. In the atmospheric context, that suggests that the original baroclinic mean zonal flow is always unstable in the presence of a small amount of Newtonian cooling. This agrees with the linear theory. As shown by WBH, an $O(\Delta)$ Newtonian cooling destabilizes and eliminates the inviscid, neutral modes (also refer to Held et al., 1985). In this regime, the dissipative role of the Newtonian cooling is relegated to longer time scales $t = O(\Delta^{-1})$ which are not accounted for in our amplitude equations.

The presence of the $O(\Delta)$ Newtonian cooling also eliminates any stationary, steady wave solution, because the coefficient of A in (3.4) becomes complex. However, a steady propagating wave solution may exist. Write

$$A = R(T)e^{i\theta(T)}$$

and convert the amplitude equations (3.3) and (3.4) to

$$\frac{d^2R}{dT^2} + \tilde{\delta}\frac{dR}{dT} - R\left(\frac{d\theta}{dT}\right)^2 - \frac{k^2C_{0I}^2}{\Delta}R + R[\tilde{\chi}(R^2 - R_0^2) + \sum_{J=1}^{\infty}\chi_J\tilde{B}_J] = 0,$$

$$\left(\frac{d}{dT} + \tilde{\delta}\right)\left(R^2\frac{d\theta}{dT}\right) = \frac{SkK^2C_{0I}^2}{2\tilde{K}\Delta^2}\mu R^2,$$

$$\frac{d\tilde{B}_J}{dT} = \frac{j^2\delta}{\Delta^{1/2}r_J}\tilde{B}_J + (\mathcal{S}_0 - G_J)\frac{dR^2}{dT}, \quad J = 1, 2, \cdots, \qquad (3.5)$$

where $R_0 = |A(0)|$. Setting $d^2R/dT^2 = dR/dT = d\tilde{B}_J/dT = 0$, but letting $d\theta/dT = \omega_e$ = constant, we find

$$\omega_e = \frac{Sk\mu}{8\tilde{K}^2\delta\Delta^{1/2}},$$

$$R_e^2 = \frac{1}{\tilde{\chi}}\left[\omega_e^2 + \frac{k^2}{4\tilde{K}(\tilde{K} - p)}\right] + R_0^2$$

$$\tilde{B}_{Je} = 0. \qquad (3.6)$$

The necessary condition for the existence of a steady wave solution requires that $\tilde{\chi} > 0$. Figure 3 displays the dependence of $\tilde{\chi}$ on the wavenumbers k and l, showing that $\tilde{\chi}$ is positive for the Green modes with meridional wavenumber $l = \pi/2$, (the gravest mode), and is small for small k but, for $l = 3\pi/2$, $\tilde{\chi}$ becomes negative for the ultralong waves. This implies that in the Regime II, the only possible steady planetary waves are those that possess the longest y-wavelength. However, in the Regime I, steady planetary waves with higher y mode ($l = 3\pi/2$) are also possible.

Although, in (3.4), steady propagating wave solutions are possible, we must test their stability to small perturbation. Write

$$R = R_e + R', \quad L = \omega_e R_e^2 + L', \quad \tilde{B}_J = \tilde{B}'_J,$$

where $L = R^2(d\theta/dT)$, and linearize (3.5) about the steady solution (3.6). For the resulting linearized equation, exponential solutions of the form

$$R', L', \tilde{B}'_J \sim (\mathcal{R}, \mathcal{L}, \mathcal{B}_J)e^{\Gamma T}$$

are possible if Γ satisfies the following algebraic equations

$$\left[\Gamma^2 + \tilde{\delta}\Gamma + 3\omega_e^2 - \frac{k^2C_{0I}^2}{\Delta} + 3\tilde{\chi}(R_e^2 - R_0^2)\right]\mathcal{R} - \frac{2\omega_e}{R_e}\mathcal{L} + R_e\sum_{J=1}^{\infty}\chi_J\mathcal{B}_J = 0, \qquad (3.7a)$$

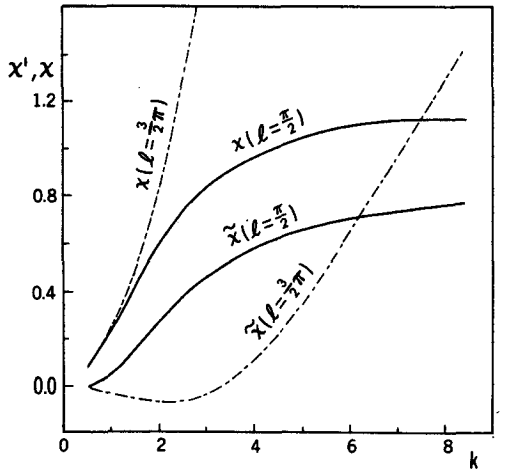

FIG. 3. Coefficients $\tilde{\chi}$ defined by (A7) and χ defined by (A5) as functions of wavenumber k for the Green modes. The solid (dot-dashed) line is calculated for $l = \pi/2$ ($l = 3\pi/2$).

$$(\Gamma + \tilde{\delta})\mathcal{L} - \mathcal{R}\mu R_e k^2 C_{0I}^2 \frac{SK^2}{\tilde{K}\Delta^2} = 0, \quad (3.7b)$$

$$\left(\Gamma - \frac{j^2\delta}{\Delta^{1/2} r_J}\right)\mathcal{B}_J = 0, \quad J = 1, 2, 3, \cdots. \quad (3.7c)$$

If

$$\Gamma = \Gamma_{1J} = \frac{j^2\delta}{\Delta^{1/2} r_J}, \quad J = 1, 2, 3, \cdots,$$

$\mathcal{B}_J$ may not be zero, and nontrivial solutions exist. Therefore, Γ_{1J} is a series of possible eigenvalues. If other eigenvalues, distinguished from Γ_{1J}, exist, $\mathcal{B}_J$ must vanish; using this fact, we obtain from the first two equations of (3.7) the following cubic equation:

$$(\Gamma + \tilde{\delta})\left[\Gamma^2 + \tilde{\delta}\Gamma + 3\omega_e^2 - \frac{k^2 C_{0I}^2}{\Delta} + 3\tilde{\chi}(R_e^2 - R_0^2)\right] - 2\mu\omega_e k C_{0I}^2 \frac{SK^2}{\tilde{K}\Delta^2} = 0. \quad (3.8)$$

Since all $\Gamma_{1J} = \delta j^2/(\Delta^{1/2} r_J) < 0$, the stability property of the steady wave solution is determined by the eigenvalues Γ_2, Γ_3, and Γ_4, which are the roots of Eq. (3.8). It can be shown that all the coefficients of the powers of Γ in (3.8) are positive real numbers, and that all the roots of (3.8) have negative real parts, indicating that when the *steady wave solutions exist, these are always stable* to small perturbations. In his study of the evolution of the Charney mode, Pedlosky (1979) showed that for Boussinesq fluids, the steady solution for $\delta = O(\Delta^{1/2})$ and $\mu = 0$ is stable for small disturbances. The result here confirms and extends Pedlosky's results for the general case.

4. Different effects of the Newtonian cooling and Ekman friction in finite amplitude dynamics

We now compare the different roles played by the two dissipative mechanisms we have considered. It can be seen from (2.2) that Ekman dissipation does not influence the vertical wave phase tilt. In the presence of an $O(\Delta^{1/2})$ Ekman dissipation, as in the inviscid case, the constant phase line tilts westward (eastward) as the amplitude increases (decreases). When the wave reaches its equilibrium state, its constant phase line becomes vertical i.e., when $dA/dT = 0$, the equilibrated wave exhibits a barotropic structure at leading order.

In contrast, the $O(\Delta^{1/2})$ internal dissipation in Regime I generates a time independent, westward phase tilt proportional to the wave amplitude and to the Newtonian coefficient, as demonstrated by (5.14) of WB. Hence the wave may still tilt westward and the horizontal heat flux may remain poleward as its amplitude decreases. When the wave reaches its steady state amplitude, the vertical wave tilt is described by

$$\frac{\partial\theta_s}{\partial z} = \frac{\mu}{k}\frac{(1 - \tilde{K}z)^2 + \tilde{K}^2 z^2}{z^2(1 - \tilde{K}z)^2 + \frac{\mu^2}{k^2}(1 - 2\tilde{K}z)^2}, \quad (4.1)$$

where θ_s represents the phase of the complex wave amplitude at steady state. Since the quantity in the rhs of (4.1) is always positive, $\partial\theta_s/\partial z > 0$, implying a westward tilt of the constant phase line. $\partial\theta_s/\partial z$ changes from k/μ at the surface to 0 at infinite height. A westward wave tilt implies that the steady wave transport heat poleward. To maintain the steady wave, conversion of zonal to eddy available potential energy is required to overcome the internal dissipation.

The characteristics of the equilibrated Green wave

TABLE 1. The characteristics of the equilibrated Green waves for different dissipative parameter (μ and δ) setting. R_e and $\bar{u}_e$ are the wave amplitude, and mean flow correction, respectively; $f_J(z)$, $\tilde{f}_J(z)$, χ and $\tilde{\chi}$ are respectively defined by (A1), (A2), (A5), and (A7).

	μ = zero	$\mu = O(\Delta)$	$\mu = O(\Delta^{1/2})$
			Regime I
δ = zero or $\delta = O(\Delta)$	$R_e = \left(R_0^2 + \frac{k^2 C_{0I}^2}{\chi\Delta}\right)^{1/2}$, $\bar{u}_e = \frac{k^2 C_{0I}^2}{\chi\Delta}\sum_{J=1}^{\infty} f_J(z)\cos jy$, No wave tilt; stationary.	Equilibration does not exist: catastrophe.	$R_e = \left(\frac{k^2 C_{0I}^2 - \mu^2}{2\chi\Delta}\right)^{1/2}$, $\bar{u}_e = \frac{(k^2 C_{0I}^2 - \mu^2)}{\chi\Delta}\sum_{J=1}^{\infty} f_J(z)\cos jy$, Wave tilts westward with height; stationary.
		Regime II	
$\delta = O(\Delta^{1/2})$	$R_e = \left(R_0^2 + \frac{k^2 C_{0I}^2}{\tilde{\chi}\Delta}\right)^{1/2}$, $\bar{u}_e = \frac{k^2 C_{0I}^2}{\tilde{\chi}\Delta}\sum_{J=1}^{\infty} \tilde{f}_J(z)\cos jy$, No wave tilt; stationary.	$R_e = \left(R_0^2 + \frac{\omega_e^2 + k^2 C_{0I}^2/\Delta}{\tilde{\chi}}\right)^{1/2}$, $\omega_e = \frac{Sk\mu}{8\tilde{k}\delta\Delta^{1/2}}$, $\bar{u}_e = \frac{\omega_e^2 + k^2 C_{0I}^2/\Delta}{\tilde{\chi}}\sum_{J=1}^{\infty} \tilde{f}_J(z)\cos jy$, No wave tilt; propagate slowly.	

for both Regimes and for five parameter settings are summarized in Table 1, where R_e and $\bar{u}_e$ are, respectively, the amplitude of the equilibrated Green wave and mean flow correction at the equilibrium state; C_{0I}, χ, $\tilde{\chi}$, $f_J(z)$ and $\tilde{f}_J(z)$ are defined by (2.5b), (A5), (A7), (A1), and (A2), respectively. Notice that, in Table 1, μ was classified into three categories, while δ fell only into two categories. This is because an $O(\Delta)$ Ekman dissipation, to $O(\epsilon)$, does not alter the equilibrated wave amplitude and the mean flow correction. There are several noticeable differences between the steady state where Ekman dissipation is the dominant energy sink, i.e., $\delta = O(\Delta^{1/2})$, and the steady state where internal dissipation (mainly Newtonian cooling) is the dominant energy sink, i.e., $\mu = O(\Delta^{1/2})$. The $O(\Delta^{1/2})$ Ekman dissipation yields a steady wave solution which depends on the initial conditions and does not depend on the magnitude of the dissipation. Since an $O(\Delta^{1/2})$ Ekman dissipation does not destroy the conservation of potential vorticity, the final equilibrium state retains its initial memory and carries no information about the dissipation. On the contrary, internal dissipation erodes the eddy potential vorticity and leads to an equilibrium state which, to leading order, does not depend on the initial amplitude but depends on the magnitude of the dissipation. The larger the internal dissipation, the smaller the equilibrium amplitude, and the smaller the mean flow correction. From (A7) it can be shown that $\tilde{\chi}$ is less than χ for all wavenumbers (also shown in Fig. 3), hence for Regime II the steady wave amplitude R_e may be significantly larger than that for the Regime I. Because of the larger amplitude of the steady waves found in Regime II, the resulting circulation resembles a "low-index" circulation, while the steady Regime I tends to resemble a "high-index" circulation. Figures 4a and 4b compare the vertical structures of the equilibrated mean flow for different latitudes and for Regimes I and II, respectively. The largest changes of the mean flow are found in the middle of the channel in both regimes. However, in Regime I, where Newtonian cooling is dominant, the mean flow is increased near the ground and decreased in the stratosphere, while in Regime II, where Ekman dissipation is dominant, the equilibrated mean flow is reduced in both the lower troposphere and the stratosphere, with the largest reductions found in the stratosphere. A comparison of $\bar{u}_e$ for Regime I and II with the $\bar{u}_e$ for the inviscid case, indicates that the presence of a dominant $O(\Delta^{1/2})$ internal dissipation reduces the amplitude but does not alter the vertical structure of the mean flow correction, while the presence of a dominant $O(\Delta^{1/2})$ Ekman dissipation not only increases the amplitude but also changes the vertical structure of the mean flow correction.

When we combine an $O(\Delta^{1/2})$ Ekman dissipation and an $O(\Delta)$ Newtonian cooling the nonlinear destabilization of the $O(\Delta)$ Newtonian cooling eliminates the stationary solution: Only a steady, propagating wave state, given by (3.6), is possible. The propagating speed of the steady wave, is determined by the ratio of μ to δ, and by the wavenumbers. The inclusion of the internal dissipation leads to a dissipation-dependent steady wave amplitude. In both regimes the steady solutions are different from the *inviscid* steady solution. Unlike the steady states in Regime I or II, the inviscid steady state is unstable to small perturbations.

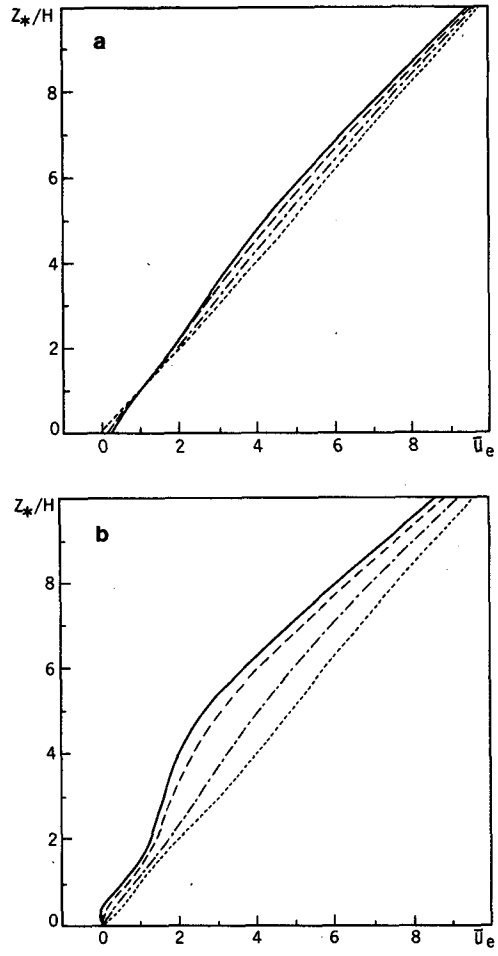

FIG. 4. The equilibrium mean flow as a function of height for the Green modes and (a) for the Regime I ($k = 1.1$, $l = \pi/2$, $\Delta = 0.1$, $2\mu/\Delta = 0.2$); (b) for the Regime II ($k = 1.1$, $l = \pi/2$, $\tilde{\delta} = 0.1$, $\Delta = 0.1$, $3\mu/\Delta = 0.03$). The solid, dashed, dot–dashed, and dotted lines are calculated at $y = 0, \pm 0.25, \pm 0.5, \pm 0.75$, respectively.

5. Stabilization of the β-effect on the finite amplitude dynamics of the planetary waves

The environmental potential vorticity gradient plays an important role in the stability of a continuous baroclinic model. Under representative winter conditions and in the presence of a representative β-effect, planetary scale waves fall in the unstable Green band ($2\tilde{K} < b < 4\tilde{K}$); however, if the β-effect were small or absent and for a nonzero basic state potential vorticity gra-

dient arising due to other effects, those waves would fall into the Charney band ($0 < b < 2\tilde{K}$).

To understand the role of the β-effect, we need to compare the Charney and Green mode dynamics for a fixed wavelength. In this section, we focus our attention on the strongly unstable *Charney* mode arising from the supercritical shear; i.e., replace $(4\tilde{K} - 2\tilde{K}\Delta)$ in Eq. (2.1) by $2\tilde{K}(1 - \Delta)$. The asymptotic solution for the total streamfunction obtained by a similar singular perturbation technique is

$$\phi(x, y, z, T) = -yz + \epsilon^{1/2}e^{pz}\left[zA(T) - i\frac{\Delta^{1/2}}{k}\frac{dA}{dT}\right] \times \cos kx \cos ly - \epsilon \sum_{J=1}^{\infty} \frac{1}{j}[\tilde{B}_J e^{r_J z} + \tilde{f}'_J(z) \times (|A|^2 - |A(0)|^2)] \sin jy + O(\epsilon^{3/2}), \quad (5.1)$$

where $A(T)$ and $\tilde{B}_J(T)$ are now governed by

$$\frac{d^2A}{dT^2} - \frac{\delta K^2}{\Delta^{1/2}p}\frac{dA}{dT} + \frac{k^2}{2\tilde{K}p}\left(1 + i\frac{\mu}{\Delta}\frac{SK^2}{2k\tilde{K}}\right)A + A[\tilde{\chi}'(|A|^2 - |A(0)|^2) + \sum_{J=1}^{\infty} \chi'_J \tilde{B}_J] = 0, \quad (5.2)$$

$$\frac{d\tilde{B}_J}{dT} = \frac{j^2\delta}{\Delta^{1/2}r_J}\tilde{B}_J - \frac{C_J}{r_J}\left[2l^2 - \frac{4l^2\tilde{K}(2p - r_J)}{(4p\tilde{K} + Sj^2)}\right]\cdot\frac{d|A|^2}{dT},$$

$$\tilde{B}_J(0) = 0. \quad (5.3)$$

As before, the wave amplitude equation has complex coefficients, i.e., in some parameter regime it is capable of exhibiting nonlinear instability. The quantity $\tilde{f}'_J(z)$, $\tilde{\chi}'$, χ'_J, C_J and r_J are given by (A3), (A8), (A9), (A4f) and (A4b), respectively. Equations (5.2) and (5.3) are the counterpart of (3.3) and (3.4) for the Charney modes. The steady propagating wave solution now becomes

$$\omega_e = \frac{\mu Sk}{4\tilde{K}^2\delta\Delta^{1/2}},$$

$$R_e^2 = R_0^2 + \frac{1}{\tilde{\chi}'}\left(\omega_e^2 - \frac{k^2}{2\tilde{K}p}\right),$$

$$\bar{u}_e = (R_e^2 - R_0^2)\sum_{J=1}^{\infty} \tilde{f}'_J(z) \cos jy. \quad (5.4)$$

The necessary condition for the existence of a steady wave solution is

$$\tilde{\chi}' > 0.$$

Figure 5 shows $\tilde{\chi}'$ as a function of wavenumber k, l for the Charney modes. It is seen that $\tilde{\chi}' < 0$ as $l = \pi/2$, $k < 1.75$, or $l = 3\pi/2$, $k < 8.40$. This is the most prominent difference between Charney and Green modes. It indicates that, according to our model, steady wave solutions are possible only for *short* waves. At 45°N, $k > 1.75$ implies that more than three waves are found along the entire latitude circle. When we take $\mu = 0$,

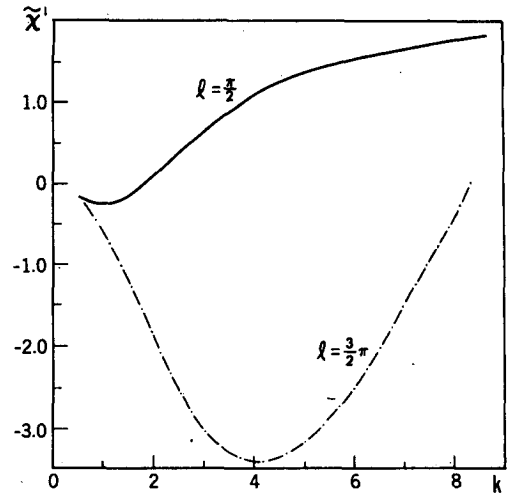

FIG. 5. Coefficient $\tilde{\chi}'$ as a function of wavenumber k for the Charney modes. The solid (dot–dashed) line is calculated for $l = \pi/2$ ($l = 3\pi/2$).

and assume the fluid to be Boussinesq, the above expressions reduce to those of Pedlosky's (1979). For typical winter shear, with the β-effect, wave two falls within the unstable Green band, i.e., in the weakly nonlinear framework this mode possesses finite amplitude stability, and the equilibrium state exists. In the absence of, or for small β, that wave falls into the Charney band, and does not possess finite amplitude stability because $\tilde{\chi}' < 0$. Therefore, the β-effect plays a stabilizing role in the weakly nonlinear dynamics of the planetary waves, and leads to an asymptotically stable equilibrium wave state.

By using a 2-layer model, Pedlosky (1981) found that even a weak β-effect leads to a dramatic change in the amplitude dynamics; as β increases, chaotic behavior gives way to more regular steady waves. His analysis was confined to a small β-parameter. The result here shows that β-effect has qualitatively similar effect on the finite amplitude waves.

If the equilibrium state exists, i.e., if $\tilde{\chi}' > 0$, the vertical structure of the equilibrium mean flow is described by the summation of $\tilde{f}'_J(z)$ at a fixed latitude. Figure 6 depicts this feature for wave six. It is seen that the existence of the steady Charney mode corrects the initial mean flow by reducing the shear in the lowest scale height. As shown in Fig. 4b, the steady Green mode, that has a large wave amplitude in the stratosphere, induces significant reduction of the initial mean shear both near the ground and in the lower stratosphere. Therefore, the reductions of the vertical shear induced by the mean flow corrections of the Charney and the Green modes, though quite different from each other, would tend to effectively eliminate their own energy source since they occur precisely where these waves draw their energy from the mean flow.

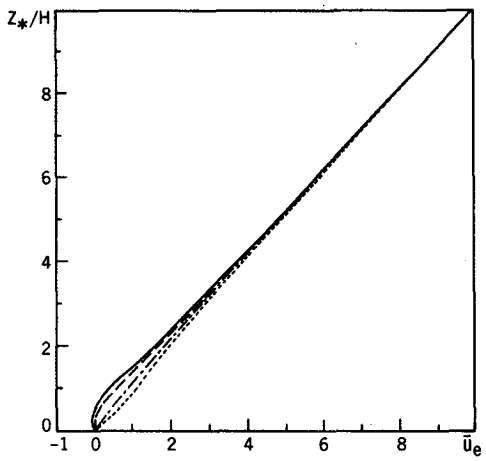

FIG. 6. The equilibrium mean flow as a function of height for the Charney modes and Regime II ($k = 3.6$, $l = \pi/2$, $\Delta = 0.1$, $\tilde{\delta} = 0.1$, $2\mu/\Delta = 0.03$). The solid, dashed, dot–dashed and dotted lines are calculated at $y = 0, \pm 0.25, \pm 0.5, \pm 0.75$, respectively.

6. Concluding remarks

We studied the different dynamic influences of the internal dissipation (mainly Newtonian cooling) and Ekman dissipation on the nonlinear evolution and equilibration by comparing the two dynamic regimes defined in section 1. In Regime II, when Ekman dissipation, $O(\Delta^{1/2})$, is dominant over Newtonian cooling, the nonlinear evolution, on a time scale of $O(\Delta^{-1/2})$, leads to a relatively large amplitude steady wave state which resembles a low index circulation pattern. Since an $O(\Delta^{1/2})$ mechanical dissipation in the boundary layer does not destroy the conservation of the interior potential vorticity, the amplitude of the steady wave depends upon initial condition and does not depend upon magnitudes of the Ekman dissipation; the steady wave exhibits a quasi-barotropic structure and does not transport heat in the meridional direction to the leading order. In sharp contrast, in Regime I, in the presence of a dominant internal thermal dissipation, a relatively small amplitude steady wave state resembling a high index circulation pattern is found. The steady wave amplitude is independent of the initial conditions but depends on the magnitudes of the internal dissipation. The steady waves in Regime I feature a baroclinic structure and transport heat poleward, the heat flux being proportional to the intensity of the internal dissipation. An $O(\Delta^{1/2})$ Ekman dissipation was also found to have a significant impact on the vertical structure of the mean flow correction.

When in isolation, i.e., in the absence of Ekman damping, a weak $O(\mu)$ Newtonian cooling prevents the nonlinear unstable Green mode from reaching an equilibrium state. This destabilization does not survive in the presence of Ekman dissipation. In Regime II, the $O(\mu)$ Newtonian cooling also changes the steady wave propagation by adding a constant eastward phase speed proportional to μ/δ.

When the dominant characteristic dissipative time scale equals the baroclinic development time scale, the evolutions of the finite amplitude waves in both regimes, on the time scale $t = O(\Delta^{-1/2})$, lead to steady (propagating or stationary) wave states, which are always stable to small perturbations. No stable limit cycle or aperiodic solutions were found in the realistic parameter ranges that typify atmospheric conditions in our model. The nonlinear stability of the baroclinic waves in the present model is found to be associated with the stabilizing effect of the planetary vorticity gradient (the β-effect). As has been shown in section 5, the change in structure in the wave amplitude from a Green to a Charney mode is responsible for negative values of $\tilde{\chi}'$, i.e., the nature of the nonlinear interaction of a finite amplitude wave with zonal mean flow is partly dependent of the vertical structure of the wave. The presence of a planetary vorticity gradient, by shifting these waves into the Green modes and thus changing the vertical structure, stabilizes the finite amplitude planetary wave circulation, and leads to an asymptotically stable equilibrium planetary wave state.

Finally, the conclusions presented are derived from the weakly nonlinear analysis which models wave–mean flow interactions but does not account for wave–wave interactions which may be dynamically important.

Acknowledgments. This material is based upon work supported, in part, by the Meteorology Program of the National Science Foundation under Grant No. ATM 8413545 and NOAA/Princeton University Grant NA84EAD00057.

APPENDIX

Expressions for Vertical Structure Functions and Wave–Mean Flow Interaction Coefficients

We denote by $f_J(z)$, $\tilde{f}_J(z)$, and $\tilde{f}'_J(z)$ the vertical structure functions of the Jth component of the mean flow corrections for the Green mode in Regime I, the Green mode in Regime II, and the Charney mode in Regime II, respectively. They are defined by

$$f_J(z) = -G_J e^{r_J z} + e^{pz}(\mathcal{S}_2 z^2 + \mathcal{S}_1 z + \mathcal{S}_0), \quad \text{(A1)}$$

$$\tilde{f}_J(z) = -\mathcal{S}_0 e^{r_J z} + e^{2pz}(\mathcal{S}_2 z^2 + \mathcal{S}_1 z + \mathcal{S}_0), \quad \text{(A2)}$$

$$\tilde{f}'_J(z) = -\frac{4l^2 \tilde{K} C_J}{4p\tilde{K} + Sj^2}(e^{2pz} - e^{r_J z}). \quad \text{(A3)}$$

In (A1) through (A3),

$$G_J = \frac{1}{r_J}(2p\mathcal{S}_0 + \mathcal{S}_1 + 2l^2 C_J), \quad \text{(A4a)}$$

$$r_J = \frac{1}{2} - \left(\frac{1}{4} + j^2 S\right)^{1/2} < 0, \quad \text{(A4b)}$$

$$\mathcal{S}_2 = \frac{8\tilde{K} l^2 C_J}{4p^2 - 2p - Sj^2}, \quad \text{(A4c)}$$

$$\mathcal{S}_1 = \frac{(2-8p)\mathcal{S}_2}{4p^2-2-Sj^2} - \frac{2\mathcal{S}_2}{\tilde{K}^2}, \tag{A4d}$$

$$\mathcal{S}_0 = \frac{\mathcal{S}_2}{\tilde{K}^2} - \frac{(4p-1)\mathcal{S}_1 + 2\mathcal{S}_2}{4p^2-2p-Sj^2}, \tag{A4e}$$

$$C_J = \frac{(-1)^{J+1}2j}{j^2-4l^2}. \tag{A4f}$$

The wave–mean flow interaction coefficients χ, $\tilde{\chi}$, χ_J, $\tilde{\chi}'$, and χ'_J, which appeared in the amplitude equations (2.5), (3.4), and (5.2), are defined by

$$\chi = \frac{\epsilon k^2}{\Delta(\tilde{K}-p)}\left\{-4\tilde{K}l^2 I_1 + \sum_{J=1}^{\infty}\frac{(-1)^J 4l^2}{j(j^2-4l^2)} \times [I_{3J} - \mathcal{S}_0 - (I_{2J}-1)G_J]\right\}, \tag{A5}$$

$$\chi_J = \frac{\epsilon k^2}{\Delta(\tilde{K}-p)}\cdot\frac{(-1)^J 4l^2}{j(j^2-4l^2)}(I_{2J}-1), \tag{A6}$$

$$\tilde{\chi} = \chi - \sum_{J=1}^{\infty}\chi_J(\mathcal{S}_0 - G_J), \tag{A7}$$

$$\tilde{\chi}' = -\frac{\epsilon k^2}{p\Delta}\left\{-\frac{2l^2K^2}{(4p-1)^2} + \sum_{J=1}^{\infty}\frac{(-1)^J 4l^2}{j(j^2-4l^2)} \times\left[\frac{-4l^2\tilde{K}C_J}{(4p\tilde{K}+Sj^2)}\left(\frac{\tilde{K}}{\tilde{K}-p}+\frac{2\tilde{K}}{r_J-2\tilde{K}}\right)\right]\right\}, \tag{A8}$$

$$\chi'_J = (-1)^J\frac{\epsilon k^2}{p\Delta}\frac{4l^2 r_J}{j(j^2-4l^2)(r_J-2\tilde{K})}. \tag{A9}$$

In (A5) through (A9),

$$I_1 = h^{-6}(h^4 + 8\tilde{K}h^3 + 36\tilde{K}^2h^2 + 96\tilde{K}^3h + 120\tilde{K}^4), \tag{A10a}$$

$$I_{2J} = -4\tilde{K}(r_J-2\tilde{K})^{-3}[(r_J-2\tilde{K})^2 + 2\tilde{K}(r_J-2\tilde{K}) + 2\tilde{K}^2], \tag{A10b}$$

$$I_{3J} = 4\tilde{K}h^{-5}[-\mathcal{S}_0h^4 + (\mathcal{S}_1 - 2\tilde{K}\mathcal{S}_0)h^3 - 2(\mathcal{S}_2 - 2\tilde{K}\mathcal{S}_1 + \tilde{K}^2\mathcal{S}_0)h^2 + 6(\tilde{K}^2\mathcal{S}_1 - 2\tilde{K}\mathcal{S}_2)h - 24\tilde{K}\mathcal{S}_2], \tag{A10c}$$

$$h = 4p - \alpha. \tag{A10d}$$

REFERENCES

Barnes, J. R., 1984: Linear baroclinic instability in the Martian atmosphere. *J. Atmos. Sci.*, **41**, 1536–1550.

Held, I. M., R. T. Pierrehumbert and R. L. Panetta, 1986: Dissipative destabilization of external Rossby waves. *J. Atmos. Sci.*, **43**, 388–396.

Leovy, C. B., 1979: Martian meteorology, *Annual Review of Astronomy and Astrophysics*, Vol. 17, Annual Reviews, 387–413.

Pedlosky, J., 1979: Finite amplitude baroclinic waves in a continuous model of the atmosphere. *J. Atmos. Sci.*, **36**, 1908–1924.

——, 1981: The effect of β on the chaotic behavior of unstable baroclinic waves. *J. Atmos. Sci.*, **38**, 717–731.

Wang, B. and A. Barcilon, 1986: The weakly nonlinear dynamics of a planetary Green mode and atmospheric vacillation. *J. Atmos. Sci.*, **43**, 1284–1296.

——, A. Barcilon and L. N. Howard, 1985: Linear dynamics of transient planetary waves in the presence of damping. *J. Atmos. Sci.*, **42**, 1893–1910.